ELSEVIER

Biophysical Chemistry 104 (2003) 121–130

Biophysical Chemistry

www.elsevier.com/locate/bpc

Water self-diffusion behavior in yeast cells studied by pulsed field gradient NMR

Ki-Jeong Suh[a], Young-Shick Hong[a], Vladimir D. Skirda[b], Vitaly I. Volkov[c], Chung-Yung Lee[a], Cherl-Ho Lee[a,*]

[a]*Graduate School of Biotechnology, Korea University, 1, 5-ka, Anam-dong, Sungbuk-ku, Seoul 136-701, South Korea*
[b]*Department of Molecular Physics, Kazan State University, Kazan, Russia*
[c]*Center of Science and High Technologies, Branch of Karpov Institute of Physical Chemistry, Moscow, Russia*

Received 20 August 2002; received in revised form 5 November 2002; accepted 5 November 2002

Abstract

The water self-diffusion behavior in yeast cell water suspension was investigated by pulsed field gradient NMR techniques. Three types of water were detected, which differ according to the self-diffusion coefficients: bulk water, extracellular and intracellular water. Intracellular and extracellular water self-diffusion was restricted; the sizes of restriction regions were approximately 3 and 15–20 μm, respectively. The smallest restriction size was determined as inner cell size. This size and also cell permeability varied with the growth phase of yeast cell. Cell size increased, but permeability decreased with increasing growth time. The values of cell permeabilities P_1^d obtained from time dependence of water self-diffusion coefficient were in good agreement with the permeabilities obtained from the exchange rate constants P_1^{eff}. The values of P_1^{eff} were 7×10^{-6}, 1.2×10^{-6} and 1.6×10^{-6} m/s, and P_1^d were 6.3×10^{-6}, 8.4×10^{-7}, 1.5×10^{-6} m/s for yeast cells incubated for 9 h (exponential growth phase), 24 h (end of exponential growth phase), and 48 h (stationary growth phase), respectively.

Keywords: Pulsed field gradient NMR; Water self-diffusion coefficient; Yeast; Growth phases

1. Introduction

Water transport in biological systems is important for cellular physiological reactions, osmotic pressure of tissue and drying process of biological materials. Transport of water in cellular system occurs either by osmotic gradient or by self-diffusional processes [1]. Osmotic water flow can be measured by monitoring changes in light scattering [2] of cell in concentration-dependent manner by fluorescence microscopy or by cell turgor pressure [3]. For diffusional water permeability, pulsed field gradient NMR (PFG-NMR) spectroscopy has become the method of choice due to its remarkable sensitivity to molecular displacements in the range of 10 nm–100 μm and to its non-invasive character [4,5].

Recently, Benga et al. [6,7] measured the diffusional water permeability of red blood cells from

*Corresponding author. Tel.: +82-2-3290-3414; fax: +82-2-927-5201.
E-mail address: chlee@korea.ac.kr (C.-H. Lee).

0301-4622/03/$ - see front matter © 2003 Elsevier Science B.V. All rights reserved.
PII: S0301-4622(02)00361-7

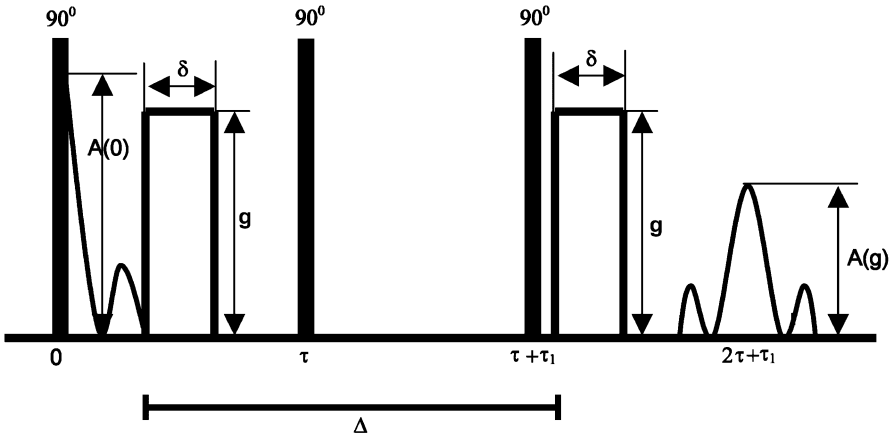

Fig. 1. Stimulated echo pulse sequence with the magnetic field gradient pulses. Here τ is the time interval between the first and second RF pulses, τ_1 is the time interval between the second and the third ones. Δ is the interval between the gradient pulses, δ is duration of the magnetic field gradient pulses, g is the amplitude of the gradient pulse. The gradient pulse is rectangular and oriented along the Z axis.

different species of animals including man by using PFG-NMR, and Waldeck et al. [8] studied the effects of cholesterol on transmembrane water diffusion in human erythrocytes by the same method. Self-diffusion of water and oil in peanuts [9], and diffusion coefficient of bound water in cotton fiber and plant tissue [10] were measured by spin-echo nuclear magnetic resonance technique. Schoberth et al. [11] measured the diffusional water permeability in *Corynebacterium glutamicum* by using home-built PFG-NMR spectrometer at a proton resonance frequency of 400 MHz with maximum field gradient amplitude of 24 T/m. With this equipment, they could reduce the observation time to less than 1 ms, which enables the measurement of self-diffusion coefficient of water in a compartment as small as a bacterial cell.

The metabolic rate and biochemical reaction in yeast cell varies with the age and environmental conditions of growth. The cell wall lysis of a thermosensitive yeast mutants is only a phenotype during the exponential growth phase [12] and the nicotinamidase activity is stimulated during the stationary growth phase by hyperosmotic shocks and ethanol treatment [13]. Also, the metabolic rate of the living cells is related to the material transport in and out of the cell and thereby could influence the permeability of the cell wall.

In the present study, we measured the self-diffusion coefficient of water in yeast cells of different growing phases by using PFG-NMR. The diffusional water permeability was estimated from the time dependence of the self-diffusion coefficient and was compared with values estimated from electron microscopy and the time dependence of compartment populations. Average cell size was estimated from the time-dependent diffusion data and was compared with electron microscopy.

The main purpose of this investigation was to understand details of yeast cell water permeability and intracellular and extracellular water molecules exchange phenomena during the process of yeast cultivation.

2. Experimental

2.1. Sample preparation

The yeast strain *Saccharomyces cerevisiae* was previously isolated from Korean rice-beer, *Takju* [14]. The activated yeast was grown in YM broth

(Difco, USA) in a shaking incubator at 27 °C. The growth curve of yeast was obtained by measuring the optical density at 600 nm of the cultivation broth. A typical sigmoid type curve obtained consisted of induction lag phase, exponential growth phase and stationary growth phase. Three types of yeast cells were investigated, the cells harvested at 9 h of incubation (MGP, mid exponential growth phase), at 24 h (EGP, end of exponential growth phase), and at 48 h (SGP, stationary growth phase), respectively. The harvested cells were centrifuged to obtain yeast pellet. It was washed 3 times with 0.1 M phosphate buffer (pH 7.0). The dry weight fraction of the pellet was 192.0 ± 3.4 mg/g, which was equivalent to 80.8% moisture content.

2.2. PFG-NMR measurement

The yeast pellet was filled in 5 mm (external diameter) NMR tube (Series 300, Aldrich Chemical, USA). The self-diffusion coefficient measurements were carried out on our home-built PFG-NMR machine, which was constructed at Center for Advanced Food Science and Technology (CAFST), Graduate School of Biotechnology, Korea University, Seoul, by Prof. Vladimir Skirda from Department of Molecular Physics, Kazan State University, Kazan, Russia. The NMR frequency for protons was 63 MHz, and the maximum field gradient amplitude was 50 T/m. The interval between magnetic field gradient pulses can vary from 2 ms to 2 s, and the duration time (δ) of magnetic field gradient pulse from 20 μs to 5 ms. The temperature of measurement was 30.0 ± 0.5 °C.

The details of PFG-NMR have been previously described in numerous references [4,5,15–18]. In our measurement we used stimulated spin-echo sequence with the magnetic field gradient pulse. This sequence is shown in Fig. 1. For molecules undergoing unhindered isotropic Brownian motion, the evolution of spin-echo amplitude is described by the following equation

$$A(2\tau,\tau_1,g) = A(2\tau,\tau_1,0)\exp(-\gamma^2 g^2 \delta^2 t_d D_s) \quad (1)$$

where γ is the gyromagnetic or magnetogyric ratio, $t_d = \Delta - \delta/3$ is the diffusion time, D_s is the self-diffusion coefficient, and τ, τ_1 and g are shown in Fig. 1. $A(2\tau, \tau_1, 0)$ is expressed by the equation

$$A(2\tau,\tau_1,0) = \frac{A(0)}{2}\exp\left(-\frac{2\tau}{T_2} - \frac{\tau_1}{T_1}\right) \quad (2)$$

where $A(0)$ is the amplitude of the signal after the first radio frequency (RF) pulse (Fig. 1). T_1 and T_2 are the spin–lattice and spin–spin relaxation time, respectively.

During the measurement of the echo signal amplitude evolution, τ and τ_1 are fixed, and only the dependence of A on g, the so-called diffusional decay is analyzed. The diffusional decay is expressed by the following equation

$$A(g) = \frac{A(2\tau,\tau_1,g)}{A(2\tau,\tau_1,0)} = \exp(-\gamma^2 g^2 \delta^2 t_d D_s) \quad (3)$$

For our PFG-NMR machine, the maximum values of g and δ are 50 T/m and 5×10^{-3} s, respectively. It allows the measurement of the diffusion coefficient from 10^{-8} to 10^{-15} m^2/s and to observe diffusional decay change in three orders of magnitude. The latter is very important when this decay is non-exponential. In the case of non-exponential decays, the experimental curve $A(g)$ is usually decomposed on the exponential components, which is described by Eq. (3). For the multi-compartment system, it consists of m-compartments (phases) in the case of slow (compare to t_d) molecular exchange between these m-compartments.

$$A(g) = \sum_{i=1}^{m} p'_i \exp(-\gamma^2 g^2 \delta^2 t_d D_{si}) \quad (4)$$

where D_{si} is the self-diffusion coefficient of ith component and

$$p'_i = p_i \exp\left(\frac{-2\tau}{T_{2i}} - \frac{\tau_1}{T_{1i}}\right) \Big/ \sum_{i=1}^{m} p_i \exp\left(\frac{-2\tau}{T_{2i}} - \frac{\tau_1}{T_{1i}}\right) \sum_{i=1}^{m} p_i = 1 \quad (5)$$

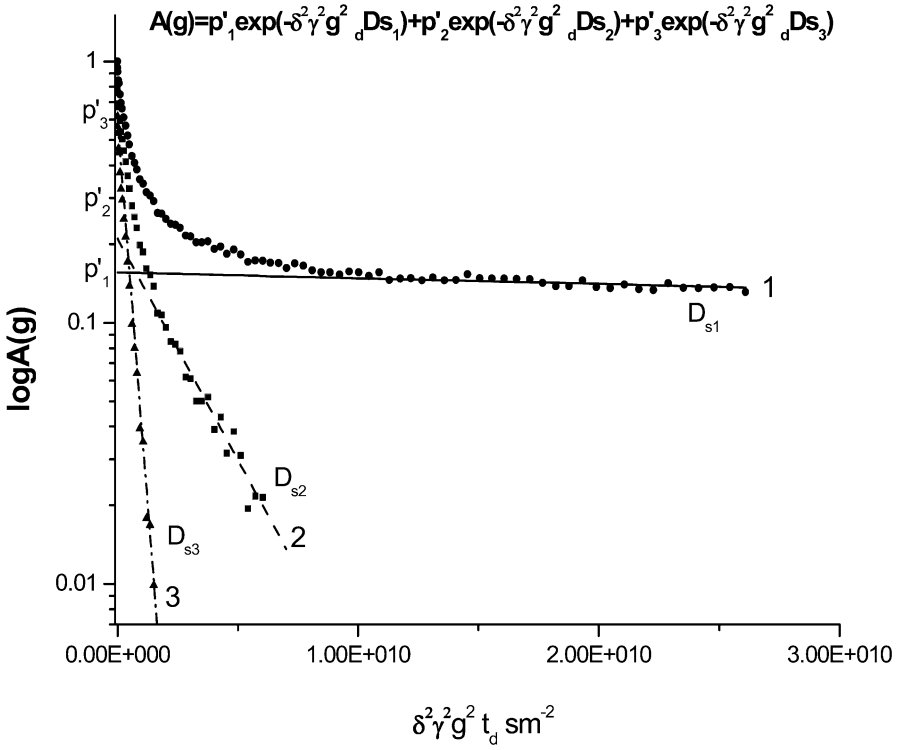

Fig. 2. The diffusional decay of water molecules in yeast incubated for 24 h (circle dots). $t_d = 400$ ms, $\delta = 100$ μs, $g_{max} = 9.65$ T/m. The accumulation number was 100. The procedures of decomposition of the original diffusional decay on three exponential components according to Eq. (4) are shown. Square and triangle dots are the result of successive subtraction of the theoretical solid-line 1 and dashed-line 2 from the original curve. Lines 1, 2 and dash-dotted-line 3 are theoretical exponential components characterized by p'_1, D_{s1}; p'_2, D_{s2} and p'_3, D_{s3}, respectively. $p'_1 = 0.16$, $D_{s1} = 5.0 \times 10^{-11}$ m^2/s; $p'_2 = 0.23$, $D_{s2} = 3.8 \times 10^{-10}$ m^2/s; $p'_3 = 0.61$, $D_{s3} = 2.6 \times 10^{-9}$ m^2/s.

p_i is the relative amount of nuclei that belongs to the molecules characterized by the self-diffusion coefficient D_{si}. The value p_i is usually called the population of ith phase. The details of the decomposition of $A(g)$ into multiple exponential components have been previously described by several research groups [17–19]. Hence, for the long T_1 and T_2 values, it is usually deduced that $p_i \approx p'_i$.

2.3. Scanning electron microscope observation

The yeast pellets were washed several times with 0.1 M phosphate buffer (pH 7.0) and fixed in 2.5% glutaraldehyde at 4 °C and postfixed in 1% OsO_4 for 2 h at room temperature. After repeated washing with 0.1 M phosphate buffer (pH 7.0), the specimens were dehydrated in graded ethanol (50%, 70%, 80%, 90%, 95% and absolute), dried in hexamethyldisilazane, and mounted on stubs. They were coated with gold using an ion sputtering coater (Eiko, IB-5, Japan) and observed with a scanning electron microscope (Hitachi, S-450, Japan) at an accelerating voltage of 15 kV.

3. Results and discussion

The typical diffusional decay of water molecules in yeast cells is shown in Fig. 2. This decay is decomposed into three exponential components, which are characterized by self-diffusion coefficients D_{s1}, D_{s2}, D_{s3} and populations p_1, p_2, p_3. D_{s3} was 2.6×10^{-9} m^2/s and is equal to the bulk water self-diffusion coefficient at 30 °C, which was measured independently. The analysis of dif-

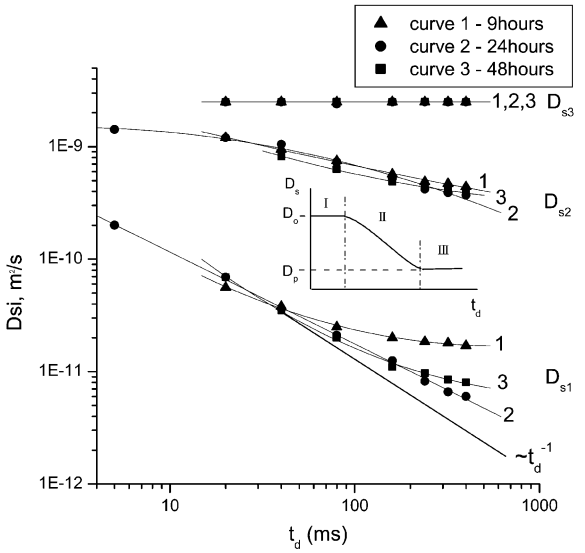

Fig. 3. The experimental dependences of water self-diffusion coefficients D_{s1}, D_{s2} and D_{s3} on diffusion time t_d for the yeast harvested after 9 h (MGP), 24 h (EGP) and 48 h (SGP) incubation curves 1, 2 and 3, respectively. The straight solid line shows dependence $D_s - t_d^{-1}$ for comparison. The insertion in figure is ideal dependence of self-diffusion coefficient on t_d in pore systems [10,20,21].

fusional decay curves at different diffusion time t_d showed that the value of populations, p_1 and p_2, and self-diffusion coefficient D_{s1} and D_{s2} depend on t_d.

The dependences of self-diffusion coefficients D_{s1}, D_{s2} and D_{s3} on diffusion time t_d are shown in Fig. 3. The values of D_{s1} and D_{s2} decreased with increasing diffusion time t_d, but D_{s3}, which is equal to bulk water self-diffusion coefficient at 30 °C was independent from t_d. The dependences $D_{s1}(t_d)$ and $D_{s2}(t_d)$ show the S-shape, which is typical for the restricted diffusion of water in pore system with permeable walls (insertion in Fig. 3). In the insertion of Fig. 3, the ideal dependence of self-diffusion coefficient D_s on t_d for the permeable pores is shown [10,20,21]. D_0 is non-restricted self-diffusion coefficient at $t_d \to 0$ in region I, and D_p is hindered self-diffusion coefficient in region III, where the total average of intrapore diffusion is achieved due to the permeability of the pore wall [20,21].

$$\frac{1}{D_p} = \frac{1}{D_0} + \frac{1}{Pa} \tag{6}$$

where P is pore wall permeability, and is the restricted size, which can be determined from the $D_s(t_d)$. In the case of nonpermeable pores, $D_s(t_d)$ is proportional to t_d^{-1} and value could be calculated from the Einstein equation

$$\langle a^2 \rangle = 6 t_d D_s \tag{7}$$

In order to take into account the permeability effect, the restriction sizes a_1 and a_2 and permeabilities P_1, and P_2 were estimated from $D_{s1}(t_d)$ and $D_{s2}(t_d)$ using the scaling approach developed by scientists [22,23], and was applied for interpretation of water self-diffusion in biological cells [9,10]. In this case the calculated dependences $D_{s1}^{eff}(t_d)$ and $D_{s2}^{eff}(t_d)$ which is proportional t_d^{-1} were analyzed, where

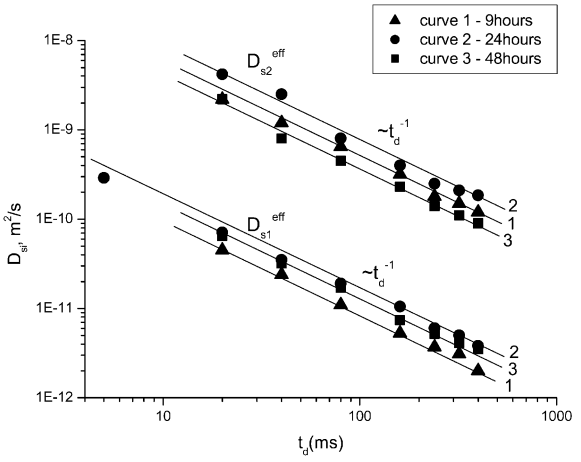

Fig. 4. The dependence of effective self-diffusion coefficient D_{s1}^{eff} and D_{s2}^{eff} on diffusion times t_d (calculated from $D_{s1}(t_d)$ and $D_{s2}(t_d)$ on Fig. 3, respectively using Eq. (8)). Yeast culture times were: 9 h—curve 1 ($D_{01} = 10^{-9}$ m^2/s, $D_{p1} = 1.5 \times 10^{-11}$ m^2/s and $D_{02} = 2 \times 10^{-9}$ m^2/s, $D_{p2} = 3.5 \times 10^{-10}$ m^2/s); 24 h—curve 2 ($D_{01} = 10^{-9}$ m^2/s, $D_{p1} = 2.5 \times 10^{-12}$ m^2/s and $D_{02} = 2 \times 10^{-9}$ m^2/s, $D_{p2} = 2.2 \times 10^{-10}$ m^2/s); 48 h—curve 3 ($D_{01} = 2 \times 10^{-9}$ m^2/s, $D_p = 4.5 \times 10^{-12}$ m^2/s and $D_{02} = 2 \times 10^{-9}$ m^2/s, $D_{p2} = 3.2 \times 10^{-10}$ m^2/s). Solid lines show the dependences which are $D_s^{eff}\mathrm{i} = A_i/t_d + B_i$, where A_i, B_i are determined by D_{0i}, D_{pi} fitting values, $i = 1, 2$.

Table 1
The values of yeast cell size a_1^n obtained from PFG-NMR, cell sizes a_1^{m}[a] and volume-to-surface ratio V_1/S_1 determined by electron microscopy, residence time τ, exchange rate constant k_1, and cell wall permeability P_1^d determined from dependence $D_{1s}(t_d)$, and permeability P_1^{eff} calculated using k_1 from $p_1(t_d)$ and V_1/S_1 from electron microscopic data

Incubation time (h)	a_1^n (μm)	a_1^m (μm)	V_1/S_1 (m)	τ (ms)	k_1 (s^{-1})	P_1^{eff} (m/s)	P_1^d (m/s)
9	2.3±0.2	4.1±1.0=a 2.9±1.0=b 3.5±1.0=$(a+b)/2$	$(1.7\pm0.3)\times10^{-6}$	240±25	4.2±0.4	$(7.0\pm0.7)\times10^{-6}$	$(6.3\pm0.6)\times10^{-6}$
24	3.0±0.2	4.9±0.5=a 3.6±0.3=b 4.2±0.4=$(a+b)/2$	$(5.4\pm0.5)\times10^{-7}$	450±40	2.2±0.2	$(1.2\pm0.1)\times10^{-6}$	$(8.4\pm0.8)\times10^{-7}$
48	2.7±0.2	4.4±0.8=a 3.8±0.8=b 4.1±0.8=$(a+b)/2$	$(7.3\pm0.7)\times10^{-7}$	400±40	2.5±0.3	$(1.6\pm0.2)\times10^{-6}$	$(1.5\pm0.2)\times10^{-6}$

[a] a_1^m was calculated as average cell size $(a+b)/2$, where a is cell size in longitudinal direction, b is the cell size in transverse direction.

$$D_s^{\text{eff}} = \frac{[D_s(t_d) - D_p]D_0}{D_0 - D_s(t_d)} \quad (8)$$

At short t_d, $D_s(t_d) \to D_0 \gg D_p$ and

$$D_s^{\text{eff}} = \frac{D_s(t_d)D_0}{D_0 - D_s(t_d)} \quad (9)$$

at long t_d, $D_s(t_d) \to D_p$ and

$$D_s^{\text{eff}} = \frac{[D_s(t_d) - D_p]D_0}{D_0 - D_p} \quad (10)$$

Eqs. (9) and (10) are usually applied for effective self-diffusion coefficient calculations [9,10,22,23]. D_0 and D_p are the fitting parameters, which are varied in order D_s^{eff} to become proportional to t_d^{-1}. From the linear dependence $D_s^{\text{eff}}(t_d)$, in which the slope is proportional to t_d^{-1}, the restricted size a is determined according to Eq. (7). The permeability was calculated from D_p value according to Eq. (6). The dependences of effective self-diffusion coefficients D_{s1}^{eff} and D_{s2}^{eff} on t_d are shown in Fig. 4. D_s^{eff} may be approximated by linear dependence on t_d^{-1}. The fitting values D_{01}, D_{02} and D_{p1}, D_{p2} are found in Fig. 4 and the calculated values a_1, a_2 and P_{1d}, P_{2d} are shown in Tables 1 and 2.

As shown in Table 1, assuming it is spherical shape of restriction, the sizes a_1^n were calculated from Einstein equation for isotropic diffusion. It was found to be approximately $1\frac{1}{2}$ times less compared to the outer sizes of yeast cells a_1^m, measured by electron microscopy (Fig. 5).

The dependences of a_1^n and a_1^m on incubation time were consistent in both measurements. It is

Table 2
The values of restricted sizes $_2$ estimated from PFG-NMR, characteristic exchange times τ, exchange rate constant k_2, characteristic permeability P_2^{eff}, calculated from $p_2(t_d)$ using k_2 and volume-to-surface ratio, suggesting spherical shape of restricting region, and permeabilities P_2^d determined from dependence $D_{s2}(t_d)$

Incubation time (h)	$_2$ (μm)	τ (ms)	k_2 (s^{-1})	P_2^{eff} (m/s)	P_2^d (m/s)
9	17±3	450±80	2.2±0.4	$(6.2\pm1.5)\times10^{-6}$	$(2.5\pm0.5)\times10^{-5}$
24	20±3	450±80	2.2±0.4	$(7.3\pm1.7)\times10^{-6}$	$(1.2\pm0.3)\times10^{-5}$
48	15±3	470±100	2.1±0.6	$(5.3\pm1.6)\times10^{-6}$	$(2.5\pm0.5)\times10^{-5}$

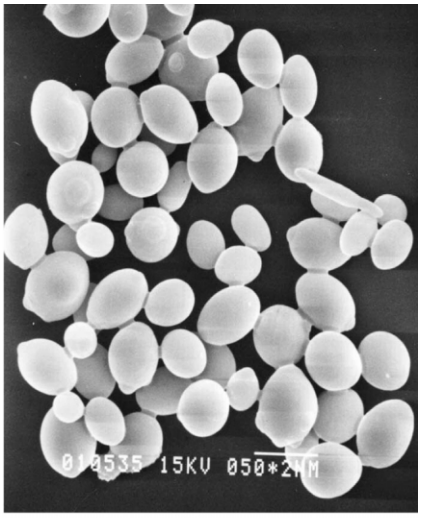

(a)

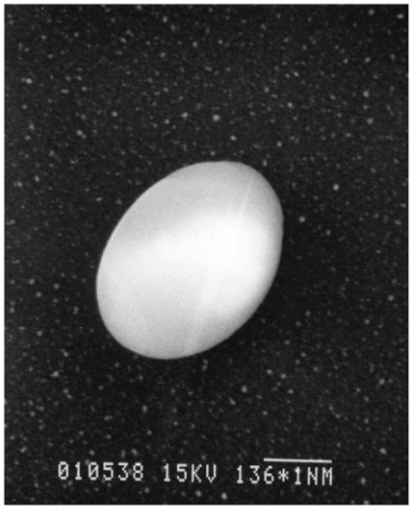

(b)

Fig. 5. SEM of *Saccharomyces cerevisiae* incubated for 48 h. Scale bar corresponds to (a) 5 μm and (b) 1.36 μm.

evident that the lowest self-diffusion coefficient D_{s1} described the water behavior in yeast cells and a_1^n the average inner size of yeast cells. From the comparison of a_1^n and a_1^m the cell wall thickness was estimated as approximately 0.5 μm. The value a_1^n agreed well with other PFG-NMR self-diffusion measurements of yeast cell size. In earlier studies it was also found that PFG-NMR sizes were less than those measured by electron microscopy [15].

The self-diffusion coefficient D_{s2}, which is approximately 1.5×10^{-9} m^2/s at $t_d\rightarrow0$, usually attributes to extracellular water diffusion. According to Waldeck et al. [5] and Schoberth et al. [11] extracellular water diffusion was obstructed. Water molecules move between cells in channels of infinite length. In this case, extracellular water self-diffusion coefficient is less compared to bulk water, but it is independent on diffusion time. In our case, the decreasing D_{s2} with increasing t_d was observed. The reasons of dependence of D_{s2} on t_d are discussed below.

Due to yeast cell walls permeability, there is molecular exchange between intracellular, extracellular and bulk water. In order to calculate water molecules residence time in the cell and the exchange rate constants, two compartments model, that implicit the exponential residence time distribution function are applied. From this model, the population of the compartment with the lowest self-diffusion coefficient D_{s1} depends on diffusion time t_d as [4]

$$p(t_d)=p(0)\exp\left(-\frac{t_d}{\tau}\right) \tag{11}$$

where τ is the water molecules residence time in the cell.

The diffusional permeability P^{eff} was calculated according to previous report [11].

$$P^{eff}=k\frac{V}{S} \tag{12}$$

where k is the molecular exchange rate constant

$$k=\frac{1}{\tau} \tag{13}$$

V/S is volume-to-surface ratio for cells. The dependences $p_1(t_d)$ are shown in Fig. 6. These dependences are in good agreement to Eq. (11). The values of cell residence time of water in the cell τ_1, exchange rate constant k_1, and permeabilities, P_1^{eff}, which were calculated from Eq. (12)

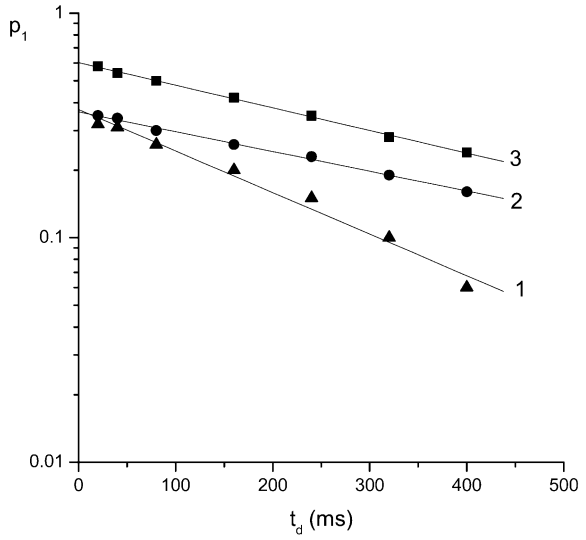

Fig. 6. The dependences of water molecules population p_1 on diffusion time t_d for yeast growing for different incubation times: (1) 9 h—LGP, (2) 24 h—EGP and (3) 48 h—SGP. Solid lines represent fits to Eq. (11).

using V/S from electron microscopic data (Table 1).

There is a good agreement between the permeabilities P_1^d, obtained from the time dependence of self-diffusion coefficient D_{s1} and the permeabilities, P_1^{eff}, which is derived from the time dependence of population $p_1(t_d)$ (Table 1). The yeast cell wall permeabilities were shown to be very sensitive to culture time. During growth, the cell wall permeability decreases about one order of magnitude from the middle exponential growth phase (9 h) to the end exponential growth phase (24 h) (Table 1).

As indicated above, the self-diffusion coefficient D_{s2}, which characterized extracellular water behavior decreased with increasing t_d. The value D_{s2}, obtained during the experiment is an apparent extracellular water self-diffusion coefficient, where intracellular and bulk water are involved because of molecular exchange. Therefore, there are two reasons of D_{s2} time dependence, the admixture of intracellular component D_{s1} into D_{s2}, and time dependence of extracellular water self-diffusion itself. As shown in Fig. 3, D_{s2} to D_{s1} ratio is over 10, and $p_1(t_d \to 0)$ and $p_2(t_d \to 0)$, which may be implicated as true populations, are nearly equal (Figs. 6 and 7). In this case, the contribution of D_{s1} into D_{s2} is negligible [11,17] and measured D_{s2} is close to true D_{s2} value. Therefore, true extracellular water self-diffusion coefficient is intrinsically time dependent and extracellular water diffusion is restricted. The size of D_{s2} restriction region a_2 and permeabilities P_2^d were also estimated by applying scaling approach. As shown in Fig. 4, $D_{s2}^{eff}(t_d)$ may be linear fitting of D_{02} and D_{p2} in Eq. (8). The calculated values a_2 and P_2 are in Table 2.

As shown in Fig. 7, $p_2(t_d)$ may be approximated by Eq. (11) and the value of water residence time in the region a_2 could be estimated. The values τ_2 and permeabilities P_2^{eff}, calculated from Eq. (12) are in Table 2. The values P_2^d and P_2^{eff} agreed to each other in the order of same magnitude, but larger disagreement was observed when compared to P_1^d and P_1^{eff}. So it may be concluded that on one hand, the two-compartments model gives opportunity for approximate estimation of residence time τ_2 only and on the other hand, V_2/S_2 was also obtained only approximately, by assuming the sphere shape of the restricting region.

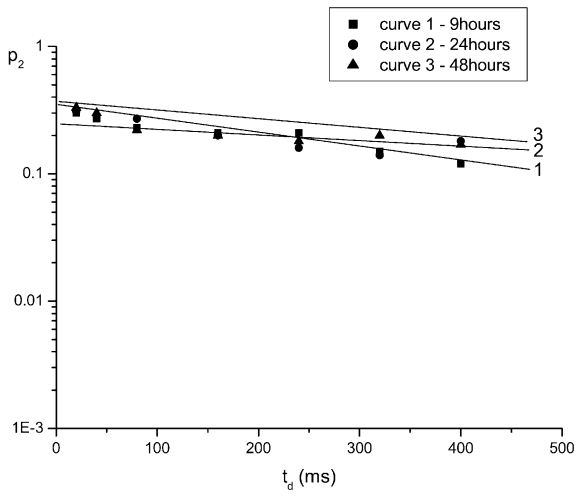

Fig. 7. The dependences of water molecules population p_2 on diffusion time t_d for yeast growth at different incubation times: 9 h—LGP, 24 h—EGP and 48 h—SGP. Solid lines represent fits to Eq. (11).

It is proposed by the authors the following reason for extracellular water restriction in this system. During sample loading in NMR tube, yeast cells forms clusters in the pellet, which restricts extracellular water self-diffusion (as shown in Fig. 5(a)). In this case, the permeability, which was estimated as P_2, characterizes the connection between clusters.

4. Conclusions

Water self-diffusion processes in yeast cells grown for different incubation times in aqueous suspension were investigated by PFG-NMR techniques. Three types of water were determined: bulk water, extracellular water and intracellular water. For both intracellular water and extracellular water, self-diffusion coefficients decreased with increasing diffusion time t_d, due to restricted diffusion.

The characteristic sizes of yeast cells a_1 and yeast cell permeabilities P_1^d depended on growth time and were 2.3, 3.0, 2.7 μm and 6.3×10^{-6}, 8.4×10^{-7}, 1.5×10^{-6} m/s for 9, 24 and 48 h of incubation, respectively. The values a_1 characterized the inner sizes of yeast cells. From the comparison of a_1 with the outer sizes of yeast cells obtained by electron microscope data, the yeast wall thickness was estimated as approximately 0.5 μm.

The residence times and rate constants of water molecular exchange were calculated. The values of permeabilities P_1 calculated from rate constants were in good agreement with the permeabilities obtained from the scaling analysis of self-diffusion coefficients time dependences.

The structural model of yeast cells distribution is proposed in study. It is suggest that yeast cells organize clusters, which restrict the external water movement. The characteristic sizes of cluster a_2 were estimated as approximately 15–20 μm. The values of permeabilities P_2, which characterize the connection between clusters, were estimated as 10^{-5} m/s.

Acknowledgments

This study was partially supported by Korea Institute of Science, Technology Evaluation and Planning (KISTEP), Republic of Korea and Russian Foundation of Basic Researches, Grant No. 00-03-32099.

References

[1] J.C. Mathai, S. Mori, B.L. Smith, et al., Functional analysis of aquaporin-1 deficient red cells, J. Biol. Chem. 271 (1996) 1309–1313.
[2] P. Agre, J.C. Mathai, B.L. Smith, G.M. Preston, Functional analyses of aquaporin water channel proteins, Methods Enzymol. 294 (1999) 550–572.
[3] T. Henzler, E. Steudle, Reversible closing of water channels in Chara internodes provides evidence for a composite transport model of the plasma membrane, J. Exp. Bot. 46 (1995) 199–209.
[4] J. Karger, H. Pheifer, W. Heink, Advances in magnetic resonance, in: J.S. Waugh (Ed.), Principles and Application of Self-diffusion Measurements by Nuclear Magnetic Resonance, vol. 12, Academic Press, New York, 1988, p. 1.
[5] A.R. Waldeck, P.W. Kuchel, A.J. Lennon, B.E. Chapman, NMR diffusion measurements to characterize membrane transport and solute binding, Progr. Nucl. Magn. Reson. Spectr. 30 (1997) 39–68.
[6] G. Benga, S.M. Grieve, B.E. Chapman, C.H. Gallagher, P.W. Kuchel, Comparative NMR studies of diffusional water permeability of red blood cells from different species. X. Camel and Alpaca, Comp. Haemat. Int. 9 (1999) 43–48.
[7] G. Benga, P.W. Kuchel, B.E. Chapman, G.C. Cox, I. Ghiran, C.H. Gallagher, Comparative cell shape and diffusional water permeability of red blood cells from Indian Elephant and Man, Comp. Haemat. Int. 10 (2000) 1–8.
[8] A.R. Waldeck, M.H. Nouri-Sorkhabi, D.R. Sullivan, P.W. Kuchel, Effects of cholesterol on transmembrane water diffusion in human erythrocytes measured using pulsed field gradient NMR, Biophys. Chem. 55 (1995) 197–208.
[9] N.L. Zakhartchenko, V.D. Skirda, R.R. Valiullin, Self-diffusion of water and oil in peanuts investigated by PFG-NMR, Magn. Reson. Imaging 16 (1998) 583–586.
[10] A.V. Anisimov, N.Y. Sorokina, N.R. Dautova, Water diffusion in biological porous systems (A NMR approach), Magn. Reson. Imaging 16 (1998) 565–568.
[11] S.M. Schoberth, N.K. Bär, R. Krämer, J. Kärger, Pulsed high-field gradient in vivo NMR spectroscopy to measure diffusional water permeability in *Corynebacterium glutamicum*, Anal. Biochem. 279 (2000) 100–105.
[12] J. Boudrant, J. De Angelo, A.J. Sinskey, S. Tannenbaum, Process characteristics of cell lysis mutants of *Saccharomyces cerevisiae*, Biotech. Bioeng. 21 (1979) 659–670.
[13] M. Ghislain, E. Talla, J.M. Francoise, Identification and functional analysis of *Saccharomyces cerevisiae* nicotamidase gene, PNCI, Yeast 19 (2002) 215–224.

[14] S.W. Yoon, C.Y.J. Lee, K.M. Kim, C.H. Lee, Leakage of cellular materials from *Saccharomyces cerevisiae* by ohmic heating, J. Microbiol. Biotechnol. 12 (2002) 183–188.

[15] J.E. Tanner, E.O. Stejskal, Restricted self-diffusion of protons in colloidal systems by the Pulsed-gradient, Spin-echo method, J. Chem. Phys. 19 (1968) 1768–1777.

[16] P.T. Callagham, Principle of NMR Microscopy, Clarendon Press, Oxford, 1991.

[17] A.I. Maklakov, V.D. Skirda, N.F. Fatkullin, Self-Diffusion in Polymer Solutions and Melts, Kazan University Press, Kazan, 1987.

[18] A.I. Maklakov, V.D. Skirda, N.F. Fatkullin, Encyclopedia of fluid mechanics, polymer flow engineering, in: N.P. Cheremisinoff (Ed.), Self-diffusion in Polymer System, vol. 9, Gult Publishing Company, Houston, 1990, p. 702.

[19] V.I. Volkov, S.A. Korotchkova, H. Ohya, Q. Guo, Self-diffusion of water–ethanol mixtures in polyacrylic acid polysulfone composite membranes obtained by pulsed-field gradient nuclear magnetic resonance spectroscopy, J. Membr. Sci. 100 (1995) 273–286.

[20] P.P. Mitra, P.N. Sen, L.M. Schawartz, Short-time behavior of the diffusion coefficient as a geometrical probe of porous media, Phys. Rev. B 47 (1993) 8565–8574.

[21] P.P. Mitra, P.N. Sen, L.M. Schwartz, P. Le Doussal, Diffusion propagator as a probe of the structure of porous media, Phys. Rev. Lett. 68 (1992) 3555–3558.

[22] R. Valiullin, V.D. Skirda, Time dependent self-diffusion coefficient of molecules in porous media, J. Chem. Phys. 114 (2001) 452–458.

[23] R.R. Valiullin, V.D. Skirda, S. Stapf, R. Kimmich, Molecular exchange processes in partially filled porous glass as seen with NMR diffusometry, Phys. Rev. E 55 (1996) 2664–2671.